Synthetic control chart with curtailment for monitoring shifts in fraction nonconforming

Salah Haridy, Nger Ling Chong, Michael B.C. Khoo, Mohammad Shamsuzzaman, Philippe Castagliola

Synthetic control chart with curtailment for monitoring shifts in fraction nonconforming

Authors' details:

1. Salah Haridy [a,b] (Corresponding Author)

   a Department of Industrial Engineering and Engineering Management, College of Engineering, University of Sharjah, Sharjah, United Arab Emirates.
   b Benha Faculty of Engineering, Benha University, Benha, Egypt.
   E-mail: sharidy@sharjah.ac.ae

2. Nger Ling Chong

   School of Mathematical Sciences, Universiti Sains Malaysia, 11800 Minden, Penang, Malaysia.
   E-mail: ngerlingc@gmail.com

3. Michael B. C. Khoo

   School of Mathematical Sciences, Universiti Sains Malaysia, 11800 Minden, Penang, Malaysia.
   E-mail: mkbc@usm.my

4. Mohammad Shamsuzzaman

   Department of Industrial Engineering and Engineering Management, College of Engineering, University of Sharjah, Sharjah, UAE.
   E-mail: mshamsuzzaman@sharjah.ac.ae

5. Philippe Castagliola

   Université de Nantes & LS2N UMR CNRS 6004, Nantes, France.
   E-mail: philippe.castagliola@univ-nantes.fr

Synthetic control chart with curtailment for monitoring shifts in fraction nonconforming

Abstract

The integration of the curtailment method with control charts considerably improves the detection speed by signaling an out-of-control condition prior to the inspection of the whole sample. To date, few research works have focused on the incorporation of the curtailment method to improve the performance of control charts. Thus, this paper incorporates the curtailment approach with the synthetic chart to propose a synthetic control chart with curtailment (Curt_Syn) for detecting upward shifts in the fraction nonconforming, p. We compared the newly developed Curt_Syn chart with the synthetic, exponentially weighted moving average (EWMA), cumulative sum (CUSUM), EWMA with curtailment (Curt_EWMA), and CUSUM with curtailment (Curt_CUSUM) charts. From an overall perspective, the results reveal that the Curt_Syn chart surpasses the synthetic chart by 38% under various conditions. For all p shifts, the Curt_Syn chart outperforms the CUSUM and EWMA charts. When the p shift is large, the Curt_Syn chart is superior to the Curt_CUSUM and Curt_EWMA charts. To demonstrate the implementation of the Curt_Syn chart, an illustrative example is provided.

Keywords: control chart; synthetic chart; curtailment; fraction nonconforming; average number of nonconforming units

Abbreviations

SPC	statistical process control
CRL	conforming run length
CUSUM	cumulative sum
EWMA	exponentially weighted moving average
ANC	average number of nonconforming units
ARL	average run length
ATS	average time to signal
VSI	variable sampling interval
VSS	variable sample size
VSSI	variable sample size and sampling interval
Curt_Syn	synthetic with curtailment
Curt_EWMA	exponentially weighted moving average chart with curtailment
Curt_CUSUM	cumulative sum with curtailment

Notation

p	fraction nonconforming
d	nonconforming units
n	sample size
$\bar{X}$	sample average
s	sample standard deviation
w	warning limit of the *np* sub-element of the synthetic chart
L	lower limit of the CRL sub-element of synthetic chart
c	cumulative number of nonconforming units
h	sampling interval
t	time required for inspecting a unit
H	upper limit of cumulative sum or exponentially weighted moving average chart
k	reference parameter of cumulative sum chart
λ	weighting parameter of exponentially weighted moving average chart
δ	size of an upward shift in fraction nonconforming
N	number of units produced per time unit
μ_δ	mean of shift in fraction nonconforming.
τ	minimum allowable value of in-control average time to signal

1. Introduction

Throughout the years, Statistical Process Control (SPC) which is a technique that aids in monitoring the behavior of a process has been widely adopted to attain a competitive advantage and an economic benefit due to the increasing competition in the manufacturing and service industries. Most companies emphasize on continuous improvement of quality, meeting the requirements of customers and reduction of cost. Hence, a control chart which is the most powerful SPC tool is a common application to monitor the stability of a process. A process can be monitored by two types of control charts, i.e. variable and attribute charts. The type of the control chart to be used is mainly decided based on the nature of the quality characteristic to be monitored. When the quality characteristic is a quantitative measure, variable charts are used. On the other hand, attribute charts are widely used for monitoring quality characteristics that cannot be

represented quantitatively or not easily expressed on a numerical scale. Each item can be categorized as either conforming or nonconforming, depending on whether the specification of the product is met. The fraction nonconforming p is defined as the ratio of the number of nonconforming items to the total number of items in a population (Montgomery, 2019). The *np* chart is used to monitor the number d of nonconforming units in a sample of size n and it is used as an alternative to the p chart when n is constant for each sample.

The conforming run length (CRL) chart was developed by Bourke (1991), where the CRL value changes with shifts in p. The CRL refers to the number of inspected samples between two consecutive nonconforming samples, including all conforming samples in between as well as the ending nonconforming sample (Wu et al. 2010). The concept of the CRL control chart is quite similar to the system proposed by Chen (1978) for monitoring congenital malformations which is based on the number of consecutive births occurring between the birth of an infant with the specific malformation being monitored and the birth of the next infant with that malformation. Such a group of consecutive births is defined as a set. Both the CRL and the size of the set proposed by Chen (1978) are random numbers and follow a geometric distribution.

The synthetic control chart was proposed by Wu et al. (2001) who combined the CRL and *np* charts to study upward shifts in fraction nonconforming. The synthetic chart uses information on the number of conforming samples between two consecutive nonconforming samples, in contrast to the *np* chart that only uses information on the number of nonconforming units in the last sample (Chong et al., 2014). Thus, it was found that the synthetic chart significantly outperforms its standard counterparts (CRL and *np* charts) in detecting p shifts. Researchers have incorporated the synthetic feature with various attribute and variable control charts. Wu and Yeo (2001) computed the average time to signal (ATS) of the synthetic control chart for attribute data. Bourke (2008) monitored the increases in fraction nonconforming with the synthetic control chart. A

synthetic-np chart was developed by Haridy et al. (2012) and they discovered that the synthetic-np chart outperforms the synthetic and *np* charts by 31% and 73%, respectively. Celano and Castagliola (2016) monitored the ratio of two normal variables using a synthetic control chart. Haq et al. (2015) proposed a synthetic control chart that detects shifts in mean and dispersion. Khoo et al. (2010) developed a synthetic double sampling control chart by integrating the synthetic and double sampling charts to monitor the process mean while the synthetic double sampling chart was proposed by Chong et al. (2014) for attribute data.

Additionally, Haq (2017) studied the synthetic exponentially weighted moving average (EWMA) and synthetic cumulative sum (CUSUM) charts with auxiliary information. In the presence of measurement errors, Hu et al. (2015) evaluated the performance of the synthetic $\bar{X}$ chart. The performance of the synthetic $\bar{X}$ chart was studied by Hu et al. (2018) when the parameters are estimated. As a considerable amount of Phase I data is required to reduce variability but is limited in practice, they used a bootstrap approach to adjust the parameters of the synthetic $\bar{X}$ chart. In terms of the median run length, Lee and Khoo (2016a) showed the outperformance of the synthetic *np* chart compared to the basic *np* chart. Meanwhile, Lee and Khoo (2016b) studied the performance of the multivariate synthetic |**s**| control chart. In a multivariate normally distributed process, the synthetic |**s**| control chart outperforms the standard |**s**| chart in detecting shifts in the covariance matrix. Shongwe and Graham (2017) combined the synthetic and runs-rules charts with the $\bar{X}$ chart. Haq (2018) proposed a nonparametric synthetic EWMA control chart while Shongwe and Graham (2016) modified the side-sensitive synthetic chart. Amdouni et al. (2016) proposed a new efficient method to monitor the coefficient of variation in a short production. Haghighati and Hassan (2018) studied the performance of control chart pattern recogniser with incomplete data and investigated the effectiveness of the exponential smoothing in restoring the patterns in order to enhance the recognition accuracy. Malela-Majika and Rapoo (2019) developed

two new synthetic double sampling charts for monitoring the location process parameter. They observed that the proposed charts have attractive zero-state and steady-state properties and outperform the existing traditional synthetic double sampling chart and all other competing charts in many situations.

The performance of a control chart can be improved through the incorporation of various approaches. An effective method to enhance a control chart's performance is by integrating the curtailment feature which has been extensively adopted in acceptance sampling plans. When the number of nonconforming units surpasses an acceptance number, practitioners stop inspecting the sample and reject the corresponding lot (Montgomery, 2019). According to Montgomery (2019), curtailment substantially reduces the average sample number used in an acceptance sampling plan. In fact, the advantage of incorporating the curtailment with control charts has been shown by various research publications. Wu et al. (2006) integrated the curtailment approach with the *np* chart and found that its performance improved significantly by decreasing the out-of-control average time to signal (ATS) by almost half in comparison with the standard *np* chart. In addition, Haridy et al. (2014) developed the CUSUM chart with curtailment which surpasses its counterpart without curtailment by 30%. While the rate of false alarm is maintained at a specified level, the incorporation of the curtailment feature into the EWMA chart by Haridy et al. (2017) has also shown a considerable improvement in the overall detection speed. The EWMA chart with curtailment was compared with the standard EWMA chart under various settings.

To the best of the authors' knowledge, a synthetic chart that incorporates the concept of curtailment is not present in the literature. Given the significant improvement of control charts through the incorporation of the curtailment approach, this paper fills this gap by proposing a synthetic control chart with curtailment to monitor *p* shifts. For brevity, the synthetic control chart with curtailment will be referred to as the Curt_Syn chart. This research focuses only on upward *p* shifts as it is more important to detect a

deterioration in quality rather than a process improvement (downward p shifts). In this paper, it is assumed that d follows a binomial distribution and the in-control value of p which is denoted as p_0 is known. The Curt_Syn chart is compared with the conventional synthetic chart, in terms of the performance measures ATS and average number of nonconforming units (ANC). The organization of this paper hereafter is as follows: Section 2 provides an overview of the synthetic control chart while the implementation of the Curt_Syn chart is outlined in Section 3. In Section 4, a discussion of the statistical measures of performance is provided while Section 5 explains the optimal design of the Curt_Syn chart. Section 6 provides the numerical analysis and an illustrative example that shows the implementation of the Curt_Syn chart is given in Section 7. Lastly, Section 8 completes the paper with conclusions and suggestions for further research.

2. Synthetic control chart

Wu et al. (2001) combined the operations of the CRL and *np* charts to develop the synthetic control chart. The CRL refers to the number of samples between two successive nonconforming samples, with the inclusion of the nonconforming sample at the end. Figure 1 illustrates three samples of the CRL, with $CRL_1 = 2$, $CRL_2 = 3$ and $CRL_3 = 4$.

[Please insert Figure 1 here]

The implementation of the synthetic chart is as follows:

(1) Determine the sample size n, warning limit w (of the *np* sub-chart) and lower control limit L (of the CRL sub-chart).

(2) Inspect a sample of n units and determine the number of nonconforming units d present in the sample.

(3) If $d \leq w$, the sample is conforming and the control flow returns to Step 2 for taking the next sample. Otherwise, if $d > w$ the sample is nonconforming and the control flow proceeds to the next step.

(4) Determine the value of CRL. If $\mathrm{CRL} \geq L$, the process is in-control and the control flow returns to Step 2. Otherwise, if $\mathrm{CRL} < L$, the process is out-of-control and the control flow proceeds to the next step.

(5) Stop the process and take corrective actions to identify and remove the assignable cause(s)

3. Curt_Syn chart

Like the synthetic chart, the implementation of the Curt_Syn chart involves the parameters *n*, *w* and *L*. For the synthetic chart, the status of a process can only be decided after inspecting all the units in a sample of size *n*. On the other hand, the Curt_Syn chart enables the detection of an out-of-control condition prior to the inspection of all *n* units in the sample. The implementation of the Curt_Syn chart can be described as follows:

(1) Identify the sample size *n*, warning limit *w* (of the *np* sub-chart) and lower control limit *L* (of the CRL sub-chart).

(2) Inspect a sample of *n* units one by one and increase the cumulative number *c* of detected nonconforming units by one whenever a nonconforming unit is found.

(3) If $c \leq w$ up to the end of the sample, the sample is conforming and return to Step 2 for taking the next sample. Otherwise, if $c > w$ at any moment, the sample is nonconforming and proceed to the next step.

(4) Determine the value of CRL. If $\mathrm{CRL} \geq L$, the process is in-control and return to Step 2. Otherwise, if $\mathrm{CRL} < L$, the process is out-of-control and proceed to the next step.

(5) Stop the process and take the necessary actions to eliminate the assignable cause(s). Subsequently, the control flow returns to Step 2.

It is worth mentioning that when d is larger than w (in the case of the synthetic chart) or c exceeds w (in the case of the Curt_Syn chart), the sample is considered as nonconforming but an out-of-control signal is not issued immediately. According to Wu et al. (2001), the sample is marked as a nonconforming one and an out-of-control signal is produced only if the CRL is less than L. In both synthetic and Curt_Syn charts, the CRL is defined as the number of samples between two consecutive nonconforming samples (including the ending nonconforming sample) as mentioned earlier.

4. Statistical measures of performance

In this section, the performance measures ATS and ANC are discussed. ATS is a widely adopted performance indicator to measure the speed of signaling an out-of-control condition. When the process is in-control, a larger ATS indicates a lower Type-I error or false alarm rate in comparison to other charts. On the other hand, a smaller out-of-control ATS indicates that the chart signals faster and is more sensitive to process shifts in comparison to other charts. In other words, a chart with a lower out-of-control ATS has a superior shift detection ability. Generally, ATS can be calculated as follows (Haridy et al., 2014):

$$\mathrm{ATS} = h \cdot \mathrm{ARL} \tag{1}$$

where h refers to the sampling interval while the average run length (ARL) is the expected number of samples until an out-of-control condition is signaled. According to Montgomery (2009), an attribute control chart based on 100% inspection of all process output is common due to the simplicity of the inspection of attribute data. Hence, 100% inspection is used in the discussions of this paper (similar to Wu et al., 2006 and Haridy et al., 2014, 2017).

The value of h is equivalent to the product of n and the time (t) required for inspecting a unit with 100% inspection. Hence, ATS is given as (Haridy et al., 2014)

$$\text{ATS} = h \cdot \text{ARL} = n \cdot t \cdot \text{ARL} \tag{2}$$

If we assume t = 1 time unit, we simply have (Haridy et al., 2017)

$$\text{ATS} = n \cdot \text{ARL} \tag{3}$$

There are two types of ATS, i.e. zero-state and steady-state ATS. The zero-state ATS is the expected time from the beginning of the process to the time when the chart signals an out-of-control condition. On the other hand, the steady-state ATS is defined as the expected time from the occurrence of an assignable cause to the time an out-of-control signal is issued by the chart. In this paper, the out-of-control ATS is computed using the steady-state mode. This is because the steady-state mode leads to more realistic results as, during the inspection of the sample, the p shift can occur randomly at any time (Wu et al., 2006). During the occurrence of a process shift, the out-of-control value of p is defined as follows (Haridy et al., 2017):

$$p = \delta \cdot p_0 \tag{4}$$

where δ measures the size of an upward shift in p, in terms of p_0. Note that $1 \le \delta \le \delta_{\max}$ such that $\delta_{\max}$ is the maximum shift. When $\delta = 1$ ($p = p_0$), the process is in the in-control state. Meanwhile, when $1 < \delta \le \delta_{\max}$, the process is out-of-control with p at its maximum $p_{\max} = \delta_{\max} \cdot p_0$.

To obtain an overall measure of the performance of the charts, the ANC which is the expected number of nonconforming units produced in various out-of-control cases, for a range of p shifts, is used. When comparing several charts, the one with a smaller ANC is more efficient over various values of the shift δ. In fact, the ANC is a weighted average of ATS, where the weight is δ. The ANC is given by (Haridy et al., 2017)

$$\text{ANC} = \text{N} \int_{1}^{\delta_{\max}} \delta \cdot p_0 \cdot \text{ATS}(\delta) \cdot f(\delta)\, \text{d}\delta \tag{5}$$

where N is the number of units produced per time unit, $f(\delta)$ represents the probability density function of δ, while $\mathrm{ATS}(\delta)$ refers to the ATS value for the shift δ. As N in Equation (5) does not affect the performance of the charts, we may assume N=1 and; hence, Equation (5) simplifies to

$$\mathrm{ANC} = \int_{1}^{\delta_{\max}} \delta \cdot p_0 \cdot \mathrm{ATS}(\delta) \cdot f(\delta)\, \mathrm{d}\delta \tag{6}$$

In general, there is no closed-form for the ANC and the value of the integral can only be obtained using a numerical method like, for instance, the Legendre-Gauss Quadrature. Additionally, note that Equation (6) (without N) can be used for the design and comparison of the charts. However, to compute the actual ANC value, Equation (5) should be used.

Typically, it is assumed that the shift δ for fraction nonconforming p follows a probability distribution. In this paper, we assume that δ follows a Rayleigh distribution. For more information on the Rayleigh distribution, readers can refer to Haridy et al. (2014, 2017). If we assume a Rayleigh distribution for the shift δ, the probability density function of δ is

$$f(\delta) = \frac{\pi(\delta - 1)}{2(\mu_\delta - 1)^2} \exp\left(-\frac{\pi(\delta - 1)^2}{4(\mu_\delta - 1)^2} \right) \tag{7}$$

and its cumulative distribution function is

$$\mathrm{F}(\delta) = 1 - \exp\left(-\frac{\pi(\delta - 1)^2}{4(\mu_\delta - 1)^2} \right) \tag{8}$$

where μ_δ is the mean of δ. The historical data corresponding to the out-of-control cases can be used to estimate μ_δ. Let $\hat{p}_i$ be the value of p obtained during the follow-up investigation after the control chart signals an out-of-control condition, then an estimate

of the sample shift $\hat{\delta}_i$ is $\hat{p}_i/p_0$. Suppose that there are k records of $\hat{\delta}_i$, i =1,...,k, then an estimation $\hat{\mu}_\delta$ of μ_δ is (Haridy et al. 2014)

$$\hat{\mu}_\delta = \frac{\sum_{i=1}^{k} \hat{\delta}_i}{k} \tag{9}$$

Note that the value of $\delta_{\max}$ in Equation (6) can be obtained from Equation (8) such that the probability of $\delta > \delta_{\max}$ is negligible (lower than 0.001). Consequently, F($\delta_{\max}$) in Equation (8) will be equal to 0.999 and $\delta_{\max}$ can be computed from μ_δ as follows:

$$0.999 = 1 - \exp\left(- \frac{\pi(\delta_{\max} - 1)^2}{4(\mu_\delta - 1)^2} \right)$$

$$\exp\left(- \frac{\pi(\delta_{\max} - 1)^2}{4(\mu_\delta - 1)^2} \right) = 0.001$$

$$- \frac{\pi(\delta_{\max} - 1)^2}{4(\mu_\delta - 1)^2} = \ln 0.001$$

giving

$$\delta_{\max} = 1 + \sqrt{\frac{-4(\mu_\delta - 1)^2 \ln 0.001}{\pi}} \tag{10}$$

5. Optimal design of the Curt_Syn chart

This section outlines the optimal design of the Curt_Syn chart with the objective of minimizing the ANC. In this paper, the design algorithm minimizes the ANC instead of the ATS to obtain a better overall detection effectiveness over a range of process shifts. It has been shown by Haridy et al. (2014) that a control chart that uses the ANC as the objective function has a better overall performance compared to its counterpart that minimizes the ATS. Prior to the optimal design of the Curt_Syn chart, three specifications should be determined:

(1) τ: minimum allowable value of the in-control ATS (ATS_0),

(2) p_0: in-control fraction nonconforming,

(3) μ_δ: mean of the shift δ.

With reference to the false alarm rate, the quality engineer can determine the value of τ. When managing false alarms is costly, a larger value of τ can be used to lower the frequency of false alarms. When the process is in-control, p_0 can be estimated from the Phase I data. Additionally, Equation (9) can be used to estimate the value of μ_δ from the historical data of the out-of-control cases.

The optimal design of the Curt_Syn chart is based on the following model:

Objective: Minimize ANC (11)

Constraint: $ATS_0 \approx \tau$ (12)

Design variables: *n, L, w*

where the objective of the model is to determine the optimal parameters *n, L* and *w* that minimize the ANC while adhering to the constraint $ATS_0 \approx \tau$. Note that the value of ATS_0 may not be exactly equal to τ due to the variability of the simulation results and the discrete characteristic of attribute data. Nevertheless, ATS_0 should be approximately equal to τ.

A two-level search is used to implement the optimal design of the Curt_Syn chart as follows:

(1) Specify the values of τ, p_0 and μ_δ.

(2) Initialize a very large number (i.e. 10^7) as the minimum value of ANC (ANC_{min}).

(3) For the first level, the optimal value of *n* is determined by trying all possible values with an increment of 1 from the initial value $n = 1$, until the ANC cannot be further reduced.

(4) For the second level, using the value of n obtained from the first level, search for the optimal value of w in the range $0 \leq w \leq n$. For each set of (n, w) values,

- Determine the value of L such that it satisfies the constraint $\text{ATS}_0 \approx \tau$.
- Given that all the values of the three charting parameters n, L and w have been determined, compute the ANC using Equation (6).
- If the computed ANC has a smaller value than $\text{ANC}_{\min}$, then substitute the latter with the former and store the current n, L and w values as a temporary optimal solution.

(5) At the end of the two-level search, the optimal Curt_Syn chart that produces the minimum ANC value and meets the constraint $\text{ATS}_0 \approx \tau$ is obtained. At the same time, the finalized optimal parameters n, L and w are determined.

The grid search used in this optimization procedure can be considered as a global one because of the discrete nature of attributes which allows all possible values of the two independent integer variables (n and w) to be explored. A code has been written in C language to compute the optimal parameters and to calculate the performance measures, ATS and ANC, of the Curt_Syn chart by simulation using 10,000 replications. This code can be obtained from the authors upon request.

6. Numerical analysis

In this section, the sensitivity of the synthetic and Curt_Syn charts in detecting upward p shifts is compared. The design of both charts follows the model in Equations (11) and (12) where the objective function is to minimize the ANC while meeting the constraint $\text{ATS}_0 \approx \tau$.

6.1 Comparison under one case

This section compares the synthetic and Curt_Syn charts under one case in which the design specifications are as shown below:

$$p_0 = 0.01,\ \tau = 50/p_0,\ \mu_\delta = 7$$

where τ is expressed in terms of p_0 (Wu et al., 2001, Wu et al., 2006). The optimal parameters of both charts are:

Synthetic chart: $n = 67$, $L = 20$, $w = 2$

Curt_Syn chart: $n = 71$, $L = 16$, $w = 2$

Table 1 shows the ATS values of both charts. The in-control ATS values are obtained when $\delta = 1$ and the out-of-control ones are obtained when $\delta = \{2,3,...,18\}$. Note that the value of $\delta_{\max}$ can be determined using Equation (10). For this case, $\delta_{\max}$ is approximately equal to 18. With reference to Table 1, it can be seen that

(1) The synthetic and Curt_Syn charts have $\text{ATS}_0 \approx \tau$ when the process is in-control. Hence, a common ground for comparison is provided as both charts have similar false alarm rates.

(2) For all shifts, the Curt_Syn chart has lower ATS values compared to the synthetic chart. Thus, the Curt_Syn chart is superior in detecting increasing p shifts as the out-of-control condition is detected earlier. From an overall viewpoint, adapting curtailment improves the effectiveness of the synthetic chart.

(3) For both charts, the ATS value decreases as δ increases. This indicates that the charts become more sensitive in detecting p shifts as δ becomes larger which is justified by the need to detect large shifts that lead to a significant loss of quality swiftly.

(4) It can also be seen from Case 0 in Table 2 that $\text{ANC}_{\text{Synthetic}}/\text{ANC}_{\text{Curt\_Syn}} = 1.43$. This reveals that the Curt_Syn chart outperforms the synthetic chart by 43% from an overall standpoint over the entire range of shifts ($1 < \delta \leq 18$).

Figure 2 shows the curves of the normalized ATS ($\text{ATS}/\text{ATS}_{\text{Curt\_Syn}}$) for both charts. The normalized ATS of the synthetic chart is more than 1 for all δ; hence for all p shifts, the Curt_Syn chart outperforms the synthetic chart. The detection ability of the synthetic

chart compared to the Curt_Syn chart worsens when the normalized ATS increases. It can be seen that the normalized ATS curve of the synthetic chart increases with δ (highest at δ = 18), indicating that the Curt_Syn chart surpasses the synthetic chart as δ increases. This is justifiable because when δ is large, the curtailment mechanism will come into play very effectively and gives an out-of-control signal much earlier before all of the n units in the sample are inspected.

[Please insert Table 1 here]

[Please insert Figure 2 here]

6.2 Comparison under more cases

In this section, the synthetic and Curt_Syn charts are compared under different conditions. As shown in Table 2 (in cases 1 to 35), there are three input factors (p_0, τ and μ_δ). p_0 has 5 levels, while τ and μ_δ are varied at 3 levels. The levels of p_0 and τ are decided with reference to those commonly used by many authors (Reynolds and Stoumbos 1998, Wu et al. 2001, Bourke 2008, Haridy et al. 2013). Case 0 corresponds to the specific case in Section 6.1. The factors varied at different levels are shown below:

p_0: 0.005, 0.03, 0.05, 0.1, 0.15

τ: $10/p_0$, $30/p_0$, $100/p_0$

μ_δ: 4, 6, 10

Note that τ is expressed in terms of p_0 as indicated in the previous section. To illustrate, if p_0 = 0.005, then $\tau = 10/p_0 = 2000$. Along with their respective charting parameters, the ANC and normalized ANC ($\mathrm{ANC} / \mathrm{ANC}_{\mathrm{Curt\_Syn}}$) values are enumerated in Table 2 for the 36 cases. It can be seen that, for all the 36 cases, the Curt_Syn chart outperforms the synthetic chart. This is because the ANC of the synthetic chart is larger than the ANC of the Curt_Syn chart for all cases. Additionally, the normalized ANC of the synthetic chart for all cases is larger than one, indicating that the Curt_Syn chart surpasses the synthetic chart. This is especially so in case 5, where the normalized ANC

of the synthetic chart is at its maximum at 1.9476. In other words, the outperformance of the Curt_Syn chart compared to the synthetic chart is 95%.

In order to obtain a complete view of the performance of the charts, a grand average of the normalized ANC for the synthetic chart in all the 36 cases shown in Table 2, denoted by $\overline{\mathrm{ANC}_{\mathrm{synthetic}} / \mathrm{ANC}_{\mathrm{Curt\_Syn}}}$, is computed. We found that $\overline{\mathrm{ANC}_{\mathrm{synthetic}} / \mathrm{ANC}_{\mathrm{Curt\_Syn}}} = 1.3785$, where the Curt_Syn chart outperforms the synthetic chart by 38%, on average in detecting p shifts. From a comprehensive point of view, the Curt_Syn chart is considerably superior to the synthetic chart. This clearly reflects the substantial contribution of the curtailment method in improving the performance of the synthetic chart.

[Please insert Table 2 here]

6.3 Comparison with CUSUM and EWMA charts with and without curtailment

Lastly, the performance of the Curt_Syn chart is compared with the CUSUM and EWMA charts, as well as their respective counterparts with curtailment, denoted as Curt_CUSUM chart and Curt_EWMA chart, respectively, for detecting increasing p shifts. We selected four different cases from Haridy et al. (2014, 2017) and studied each case in terms of the ANC. Table 3 shows the design specifications, optimal parameters and results of each case. Note that H is the upper control limit of the CUSUM and EWMA charts, k is the reference parameter of the CUSUM chart and λ is the weighting parameter of the EWMA chart.

[Please insert Table 3 here]

Based on Table 3, the Curt_Syn chart outperforms the CUSUM and EWMA charts for all cases as the CUSUM and EWMA charts' normalized ANC values are more than one. In fact, the Curt_Syn chart significantly outperforms the CUSUM and EWMA charts when p_0 is large ($p_0 = 0.03$). The Curt_Syn chart surpasses the synthetic chart for all cases. Meanwhile, the Curt_Syn chart also outperforms the Curt_CUSUM and Curt_EWMA charts when p_0 is large.

It can also be seen that, generally, the Curt_CUSUM and Curt_EWMA charts are slightly superior to the Curt_Syn chart when p_0 is small ($p_0 = 0.005$). However, as the synthetic chart without curtailment has larger ANC values compared to the Curt_CUSUM and Curt_EWMA charts for all cases (except for case 4 where the Curt_CUSUM chart has a larger ANC value), the incorporation of the curtailment method has improved the performance of the synthetic chart significantly. To illustrate, in case 2, the synthetic chart has ANC = 11.564 which decreases to ANC = 7.496 for the Curt_Syn chart, which is closer to the performance of the Curt_CUSUM (ANC = 7.865) and Curt_EWMA (ANC = 7.459) charts. It can also be observed in case 3 that the addition of the curtailment approach to the synthetic chart reduced its ANC from 5.147 to 3.286; hence outperforming the Curt_CUSUM (ANC = 4.441) and Curt_EWMA (ANC = 4.332) charts.

7. Illustrative example

The implementation of the Curt_Syn chart in a company that manufactures golf balls is shown in this example. A golf ball is considered nonconforming if the label on the golf ball is printed wrongly. As the quality engineer is only interested in process deterioration, only upward shifts in p are monitored. Based on the Phase I dataset, the p_0 value is estimated as 0.01. The mean value μ_δ of the random shift δ is estimated as 5, based on some investigation records of the out-of-control cases. The quality engineer has also set the allowable minimum $\tau = 6000$. The value of $\delta_{\max}$ is 12 when $\mu_\delta = 5$ according to Equation (10). Using the optimization program, the optimal parameters, ANC and normalized ANC of the two charts are as follows:

Synthetic chart: $n = 67$, $L = 16$, $w = 2$, ANC = 6.3380, $\text{ANC}_{\text{Syn}}/\text{ANC}_{\text{Curt\_Syn}} = 1.2283$

Curt_Syn chart: $n = 62$, $L = 23$, $w = 2$, ANC = 5.1598

[Please insert Table 4 here]

[Please insert Figure 3 here]

It can be seen from Table 4 that the Curt_Syn chart is superior to the synthetic chart for all shifts. From an overall point of view, the Curt_Syn chart outperforms the synthetic chart by 23%. Additionally, Figure 3 shows that the curve of the Curt_Syn chart is lower than the synthetic chart; thus the Curt_Syn chart has lower ATS values and it is more sensitive for detecting p shifts. Using the Curt_Syn chart, 20 samples, each with size $n = 62$ are selected. Table 5 shows the cumulative number c of detected nonconforming units and the status of the samples while Figure 4 shows the implementation of the Curt_Syn chart. For each sample, the 62 units are inspected one by one and c is increased by one when a nonconforming unit is found. At sample #17, $c = 5$ exceeds $w = 2$, thus, the sample is nonconforming. As CRL = 17 does not exceed $L = 23$, an out-of-control condition is signaled at sample #17. Hence, the quality engineer stops the process to take corrective actions.

[Please insert Table 5 here]

[Please insert Figure 4 here]

8. Conclusions

In this paper, we propose a new synthetic chart with curtailment which is abridged as the Curt_Syn chart. The performance of the Curt_Syn chart is comprehensively studied in this paper for various conditions, in terms of ATS and ANC to provide readers with an overall view of the performance of the chart. Additionally, the implementation, optimal design and performance evaluation of the Curt_Syn chart are explained to assist practitioners in using the chart.

The curtailment method can be easily applied and has significantly improved the performance of the synthetic chart by 38%, in terms of ANC. The Curt_Syn chart also outperforms the CUSUM and EWMA charts, in terms of ANC. In addition, the Curt_Syn chart surpasses the Curt_CUSUM and Curt_EWMA charts for large p shifts. When p shifts occur, an out-of-control condition will be signaled by the Curt_Syn chart before the

inspection of all the n units in a sample; consequently, an improvement in the speed of detecting p shifts is attained.

As the Curt_Syn chart is studied based on 100% inspection in this paper, further research can investigate the Curt_Syn chart's performance for uniform or random sampling inspection. In addition, the performance of the adaptive (i.e. variable sampling interval (VSI), variable sample size (VSS) and variable sample size and sampling interval (VSSI)) charts can be improved with the addition of curtailment. Further research can also be done on the incorporation of the curtailment technique with multiattribute charts.

Acknowledgements

The authors sincerely thank the editor and reviewers for their constructive suggestions and valuable comments that led to a substantial improvement of the paper. This research is supported by the University of Sharjah, UAE, under Competitive Research Project No. 18020405112.

References

Amdouni A., Castagliola P., Taleb H., Celano G. (2016) One-sided run rules control charts for monitoring the coefficient of variation in short production runs. *European Journal of Industrial Engineering*, 10(5), 639-663

Bourke P. D. (1991). Detecting a shift in fraction nonconforming using run-length control charts with 100% inspection. *Journal of Quality Technology*. 23(3), 225–238.

Bourke P. D. (2008). Performance comparisons for the synthetic control chart for detecting increases in fraction nonconforming. *Journal of Quality Technology*, 40(4), 461–475.

Celano G. & Castagliola P. (2016). A synthetic control chart for monitoring the ratio of two normal variables. *Quality and Reliability Engineering International*, 32(2), 681-696.

Chen R. (1978): A surveillance system for congenital malformations. *Journal of the American Statistical Association*, 73:362, 323-327.

Chong Z.L., Khoo M. B. C. & Castagliola P. (2014). Synthetic double sampling np control chart for attributes. *Computers & Industrial Engineering*, 75, 157–169.

Haghighati R., Hassan A. (2018) Recognition performance of imputed control chart patterns using exponentially weighted moving average. *European Journal of Industrial Engineerin*g, 12 (5), 637 – 660.

Haq A. (2017). New synthetic CUSUM and synthetic EWMA control charts for monitoring the process mean using auxiliary information. *Quality and Reliability Engineering International*, 33(7), 1549-1565.

Haq A. (2018). A new nonparametric synthetic EWMA control chart for monitoring process mean. *Communications in Statistics-Simulation and Computation*, 1-12. DOI:10.1080/03610918.2017.1422750

Haq A., Brown J. & Moltchanova E. (2015). New synthetic control charts for monitoring process mean and process dispersion. *Quality and Reliability Engineering International*, 31(8), 1305-1325.

Haridy S., Rahim M. A., Selim S. Z., Wu Z. & Benneyan J. C. (2017) EWMA chart with curtailment for monitoring fraction nonconforming. *Quality Technology & Quantitative Management*, 14(4), 412-428.

Haridy S., Wu Z., Chen S. & Knoth S. (2014). Binomial CUSUM chart with curtailment. *International Journal of Production Research*, 52(15), 4646-4659.

Haridy S., Wu Z., Khoo M. B. C. & Yu F. J. (2012). A combined synthetic and np scheme for detecting increases in fraction nonconforming. *Computers & Industrial Engineering*, 62(4), 979–988.

Haridy S., Wu Z., Yu F. J. and Shamsuzzaman M. (2013) An optimization design of the combined np-CUSUM scheme for attributes. *European Journal of Industrial Engineering*, 7(1), 16-37.

Hu X., Castagliola P., Ma Y. & Huang W. (2018). Guaranteed in-control performance of the synthetic $\bar{X}$ chart with estimated parameters. *Quality and Reliability Engineering International*, 34(5), 759-771.

Hu X., Castagliola P., Sun J. & Khoo M. B. C. (2015). The effect of measurement errors on the synthetic $\bar{X}$ chart. *Quality and Reliability Engineering International*, 31(8), 1769-1778.

Khoo M. B. C., Lee H. C., Wu Z., Chen C. H. & Castagliola P. (2010). A synthetic double sampling control chart for the process mean. *IIE Transactions*, 43(1), 23–38.

Lee M. H. & Khoo M. B. C. (2016a). Optimal design of synthetic np control chart based on median run length. *Communications in Statistics-Theory and Methods*, 46(17), 8544-8556.

Lee M. H. & Khoo M. B. C. (2016b) Optimal designs of multivariate synthetic **|S|** control chart based on median run length. *Communications in Statistics-Theory and Methods*, 46(6), 3034-3053.

Malela-Majika j., Rapoo E. (2019) Side-sensitive synthetic double sampling X control charts. *European Journal of Industrial Engineering*, 13(1), 117-148

Montgomery D.C. (2009). *Introduction to Statistical Quality Control* (6th edn.). New York: John Wiley & Sons.

Reynolds M. R., Stoumbos Z. G. (1998) The SPRT chart for monitoring a proportion. *IIE Transactions*, 30(6), pp. 545-561.

Shongwe S. C. & Graham M. A. (2016). A modified side-sensitive synthetic chart to monitor the process mean. *Quality Technology & Quantitative Management*, 15(3), 328-353.

Shongwe S. C. & Graham M. A. (2017). Synthetic and runs-rules charts combined with an $\bar{X}$ chart: theoretical discussion. *Quality and Reliability Engineering International*, 33(1), 7-35.

Wu Z. & Yeo S. H. (2001). Implementing synthetic control charts for attributes. *Journal of Quality Technology,* 33(1), 112–114.

Wu Z., Luo H. & Zhang X. (2006). Optimal np control chart with curtailment. *European Journal of Operational Research*, 174(3), 1723-1741.

Wu Z., Wang Z., Jiang W. (2010) A generalized conforming run length control chart for monitoring the mean of a variable. *Computers and Industrial Engineering*, 59(2), 185-192.

Wu Z., Yeo S. H., Spedding T. A. (2001). A synthetic control chart for detecting fraction nonconforming increases. *Journal of Quality Technology*, 33(1), 104–111.

Table 1: ATS values of the synthetic and Curt_Syn charts for the specific case

	ATS	
δ	Synthetic	Curt_Syn
1	5123.611	4901.927
2	507.787	495.920
3	210.200	183.360
4	133.934	104.543
5	102.719	73.772
6	82.491	56.530
7	71.430	45.623
8	62.653	38.800
9	57.232	33.983
10	52.757	29.987
11	48.817	26.953
12	45.956	25.013
13	43.236	22.847
14	41.621	21.181
15	39.799	20.067
16	39.062	18.435
17	38.412	17.442
18	37.615	16.487

Table 2: Comparison of the synthetic and Curt_Syn charts under different levels of p_0, τ and μ_δ

Case	p_0	τ	μ_δ	Chart	n	L	w	ANC	ANC/ANC$_{\text{Curt_Syn}}$
0	0.01	50/p_0	7	Synthetic	67	20	2	5.6048	1.4295
				Curt_Syn	71	16	2	3.9207	1.0000
1	0.005	10/p_0	4	Synthetic	1	22	0	4.2733	1.3025
				Curt_Syn	70	27	1	3.2808	1.0000
2	0.005	10/p_0	10	Synthetic	1	22	0	2.7678	1.2094
				Curt_Syn	75	21	1	2.2886	1.0000
3	0.005	10/p_0	6	Synthetic	1	22	0	3.4452	1.2790
				Curt_Syn	77	20	1	2.6936	1.0000
4	0.005	100/p_0	4	Synthetic	49	5	1	12.7656	1.6430
				Curt_Syn	112	19	2	7.7698	1.0000
5	0.005	100/p_0	10	Synthetic	38	9	1	7.5626	1.9476
				Curt_Syn	111	19	2	3.8830	1.0000
6	0.005	100/p_0	6	Synthetic	49	5	1	9.2602	1.7490
				Curt_Syn	111	19	2	5.2946	1.0000
7	0.005	30/p_0	4	Synthetic	40	29	1	7.6711	1.6349
				Curt_Syn	162	17	2	4.6921	1.0000
8	0.005	30/p_0	10	Synthetic	40	29	1	4.3554	1.2698
				Curt_Syn	40	29	1	3.4299	1.0000
9	0.005	30/p_0	6	Synthetic	40	29	1	5.6335	1.5286
				Curt_Syn	185	10	2	3.6853	1.0000
10	0.03	10/p_0	4	Synthetic	12	28	1	3.5987	1.2811
				Curt_Syn	108	4	3	2.8090	1.0000
11	0.03	10/p_0	10	Synthetic	1	4	0	2.6398	1.2205
				Curt_Syn	13	21	1	2.1628	1.0000
12	0.03	10/p_0	6	Synthetic	12	28	1	3.3596	1.2825
				Curt_Syn	13	21	1	2.6195	1.0000
13	0.03	100/p_0	4	Synthetic	39	18	3	8.3399	1.2792
				Curt_Syn	109	4	5	6.5194	1.0000
14	0.03	100/p_0	10	Synthetic	22	11	2	5.5922	1.5480
				Curt_Syn	20	16	2	3.6126	1.0000
15	0.03	100/p_0	6	Synthetic	20	16	2	6.3430	1.2546
				Curt_Syn	40	16	3	5.0559	1.0000
16	0.03	30/p_0	4	Synthetic	30	12	2	5.6705	1.2953
				Curt_Syn	105	4	4	4.3777	1.0000
17	0.03	30/p_0	10	Synthetic	25	28	2	5.1487	1.8023
				Curt_Syn	31	10	2	2.8567	1.0000
18	0.03	30/p_0	6	Synthetic	30	12	2	5.1858	1.4672
				Curt_Syn	31	10	2	3.5345	1.0000

Table 2 (continued)

Case	p_0	τ	μ_δ	Chart	n	L	w	ANC	ANC/ANC$_{\text{Curt_syn}}$
19	0.05	10/p_0	4	Synthetic	8	21	1	3.6419	1.2702
				Curt_Syn	64	4	3	2.8672	1.0000
20	0.05	10/p_0	10	Synthetic	1	3	0	2.5690	1.1579
				Curt_Syn	8	21	1	2.2186	1.0000
21	0.05	10/p_0	6	Synthetic	1	3	0	3.2734	1.2462
				Curt_Syn	8	21	1	2.6267	1.0000
22	0.05	100/p_0	4	Synthetic	12	19	2	8.2075	1.2463
				Curt_Syn	63	5	5	6.5854	1.0000
23	0.05	100/p_0	10	Synthetic	13	13	2	5.6036	1.4755
				Curt_Syn	12	19	2	3.7978	1.0000
24	0.05	100/p_0	6	Synthetic	12	19	2	6.2001	1.2228
				Curt_Syn	28	7	3	5.0703	1.0000
25	0.05	30/p_0	4	Synthetic	18	13	2	5.6006	1.2686
				Curt_Syn	39	6	3	4.4148	1.0000
26	0.05	30/p_0	10	Synthetic	18	13	2	5.3955	1.7824
				Curt_Syn	18	13	2	3.0272	1.0000
27	0.05	30/p_0	6	Synthetic	18	13	2	5.1378	1.4340
				Curt_Syn	19	10	2	3.5828	1.0000
28	0.1	30/p_0	4	Synthetic	9	16	2	5.3494	1.2192
				Curt_Syn	10	9	2	4.3877	1.0000
29	0.1	30/p_0	10	Synthetic	9	16	2	4.9890	1.4772
				Curt_Syn	9	16	2	3.3773	1.0000
30	0.1	100/p_0	4	Synthetic	7	13	2	7.7125	1.2086
				Curt_Syn	32	5	5	6.3812	1.0000
31	0.1	100/p_0	10	Synthetic	6	30	2	5.3246	1.3181
				Curt_Syn	7	13	2	4.0396	1.0000
32	0.15	30/p_0	4	Synthetic	6	21	2	4.8768	1.2190
				Curt_Syn	13	7	3	4.0005	1.0000
33	0.15	30/p_0	10	Synthetic	2	26	1	4.1410	1.0741
				Curt_Syn	6	21	2	3.8553	1.0000
34	0.15	100/p_0	4	Synthetic	5	13	2	7.2179	1.2043
				Curt_Syn	15	8	4	5.9935	1.0000
35	0.15	100/p_0	10	Synthetic	2	7	1	7.5150	1.3776
				Curt_Syn	10	7	3	5.4553	1.0000

Table 3: Comparison with the CUSUM and EWMA charts with and without curtailment

Case	p_0	τ	μ_δ	Chart	n	L	w	H	k or λ	ANC	ANC/ANC$_{Curt_Syn}$
1	0.005	1000	3	EWMA	56	-	-	0.511	0.53	2.944	1.010
				CUSUM	84	-	-	0.242	0.88	2.991	1.026
				Synthetic	2	23	0	-	-	3.141	1.077
				Curt_EWMA	80	-	-	0.432	0.47	2.697	0.925
				Curt_CUSUM	83	-	-	0.368	0.84	2.669	0.915
				Curt_Syn	50	2	0	-	-	2.916	1.000
2	0.005	10000	3	EWMA	54	-	-	0.239	0.08	8.048	1.074
				CUSUM	76	-	-	2.702	0.66	8.570	1.143
				Synthetic	64	5	1	-	-	11.564	1.543
				Curt_EWMA	84	-	-	0.064	0.02	7.459	0.995
				Curt_CUSUM	112	-	-	2.910	0.87	7.865	1.049
				Curt_Syn	141	16	2	-	-	7.496	1.000
3	0.03	1000	7	EWMA	63	-	-	1.083	0.50	7.637	2.324
				CUSUM	62	-	-	1.060	2.97	8.059	2.452
				Synthetic	30	12	2	-	-	5.147	1.566
				Curt_EWMA	50	-	-	1.138	0.50	4.332	1.318
				Curt_CUSUM	69	-	-	0.861	3.14	4.441	1.351
				Curt_Syn	30	12	2	-	-	3.286	1.000
4	0.03	10000	7	EWMA	50	-	-	2.106	0.50	11.375	1.945
				CUSUM	66	-	-	3.961	3.02	12.112	2.071
				Synthetic	14	27	2	-	-	7.896	1.350
				Curt_EWMA	53	-	-	2.125	0.50	7.853	1.343
				Curt_CUSUM	71	-	-	3.239	3.76	8.160	1.395
				Curt_Syn	33	14	3	-	-	5.848	1.000

Table 4: ATS values of the Synthetic and Curt_Syn charts corresponding to the golf ball manufacturing process

δ	Synthetic	Curt_Syn
1	6108.4034	6053.5346
2	593.2122	535.6702
3	217.5566	201.5670
4	135.7697	114.9303
5	101.8074	80.9814
6	83.4829	58.9744
7	71.3157	47.9615
8	63.9055	40.1599
9	57.1117	34.7150
10	52.2140	30.3919
11	48.8171	27.3797
12	45.6547	24.5865

Table 5: Phase II dataset from the golf ball manufacturing process

Sample	c	Status
1	1	Conforming
2	2	Conforming
3	1	Conforming
4	0	Conforming
5	1	Conforming
6	1	Conforming
7	1	Conforming
8	0	Conforming
9	1	Conforming
10	2	Conforming
11	2	Conforming
12	1	Conforming
13	1	Conforming
14	0	Conforming
15	0	Conforming
16	0	Conforming
17	5	Nonconforming
18	0	Conforming
19	1	Conforming
20	0	Conforming

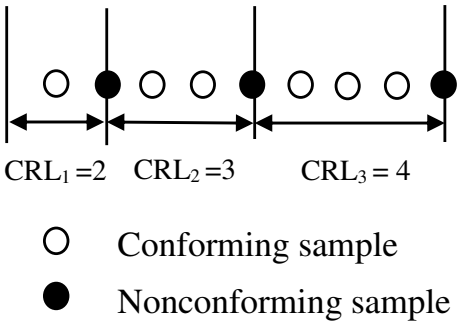

Figure 1: Example of conforming run length (CRL)

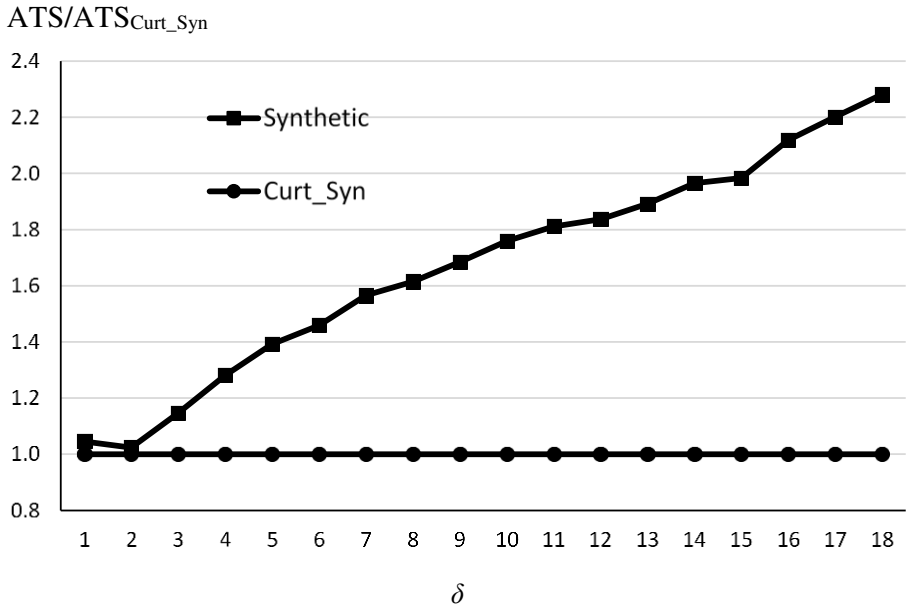

Figure 2: Normalized ATS of the synthetic and Curt_Syn charts for the specific case

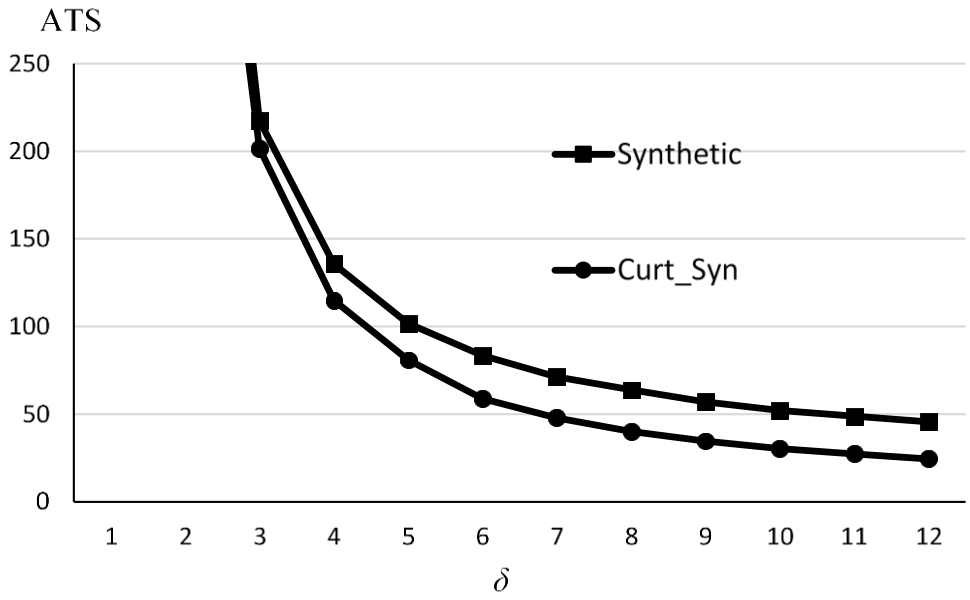

Figure 3: ATS values of the synthetic and Curt_Syn charts corresponding to the golf ball manufacturing process

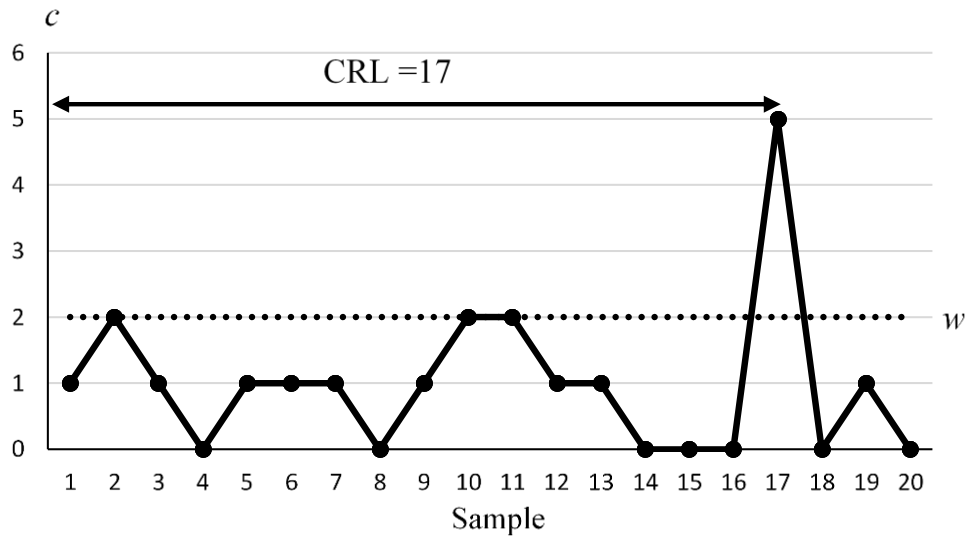

Figure 4: The Curt_Syn chart corresponding to the golf ball manufacturing process